Electronic Supplementary Material (ESI) for Materials Horizons

Supplementary Information

Lithium-ion storage properties of titanium oxide nanosheets

Veronica Augustyn,[a,b] Edward R. White,[b,c] Jesse Ko,[a,b] George Grüner,[b,c]

Brian C. Regan,[b,c] and Bruce Dunn[a,b,*]

[a]Department of Materials Science and Engineering, University of California, Los Angeles, CA 90095 USA

[b]California NanoSystems Institute, University of California, Los Angeles, CA 90095 USA

[c] Department of Physics and Astronomy, University of California, Los Angeles, CA 90095 USA

[*]Corresponding author; bdunn@ucla.edu

Experimental methods

1. Synthesis

The solvothermal synthesis of anatase TiO_2 NS with exposed {001} facets has been reported previously (B. Wu, C. Guo, N. Zheng, Z. Xie, and G.D. Stucky. *J. Am. Chem. Soc*, 2008, **130**, 17563). Briefly, 5 mL of benzyl alcohol, 2 mL of oleylamine, and 0.25 mL of titanium isopropoxide are sealed in a Teflon-lined autoclave and heated at 180°C for 1 day. The resulting solution is centrifuged and the white precipitates washed with alternating cycles of chloroform and ethanol. The addition of a small amount of water to the reaction (60 µL) leads to the growth of anatase NCs. To yield dispersions in ethanol, 100 mg of TiO_2 went through a 7 day exfoliation process in a solution of 400 mg of tetrabutylammonium hydroxide in 20 mL of ethanol, in order to replace the oleylamine. For electrochemical measurements, the concentration of TiO_2 in ethanol was 1 mg mL^{-1}.

2. Characterization

Electrochemical behavior was investigated using drop-cast films (~20 µg cm^{-2}) of NS and NCs on stainless steel. The three-electrode measurements were performed with lithium metal counter and reference electrodes and 1 M $LiClO_4$ in propylene carbonate (PC) as the electrolyte. For the Na-ion experiments, the cell consisted of sodium metal counter and reference electrodes and 1 M $NaClO_4$ in PC as the electrolyte. Cyclic voltammetry was performed from 1 to 100 mV s^{-1} between 1 and 3 V (*vs*. Li/Li^+ or Na/Na^+) using a PAR EG&G 273 potentiostat. All electrochemical cells were tested in an argon-filled glovebox with H_2O and O_2 levels < 1 ppm.

Powder X-ray diffraction (XRD) was performed on the Rigaku Miniflex II with a Cu K_α X-ray source. X-ray photoelectron spectroscopy (XPS) measurements were taken with the Kratos AXIS Ultra using a monochromated Al X-ray source at 10 mA and 15 kV and a 20 eV pass energy. XPS of cycled electrodes was performed by rinsing the samples with dimethyl carbonate (DMC) and loading them into an inert atmosphere transfer chamber, which was then connected directly to the XPS chamber. All XPS spectra were calibrated to the C 1s peak at 284.9 eV and peak fitting was performed with the Casa XPS program using a 70:30 Gaussian-Lorentzian lineshape. Transmission electron microscopy (TEM) was performed with the JEOL JEM 1200-EX. TEM of cycled NS material was performed by drop-casting a small amount of NS in ethanol onto a Cu TEM grid, which was then used as the working electrode in the electrochemical cell. Cyclic voltammetry was performed for 6 cycles at 10 mV s^{-1} between 1 and 3 V, then the grid was rinsed with DMC and transferred under an inert atmosphere into the TEM with minimal ambient atmosphere exposure. High resolution TEM (HR TEM) was performed with the FEI Titan 80/300 kV S/TEM under various conditions, as described in Figures S3, S4, S5, and S6.

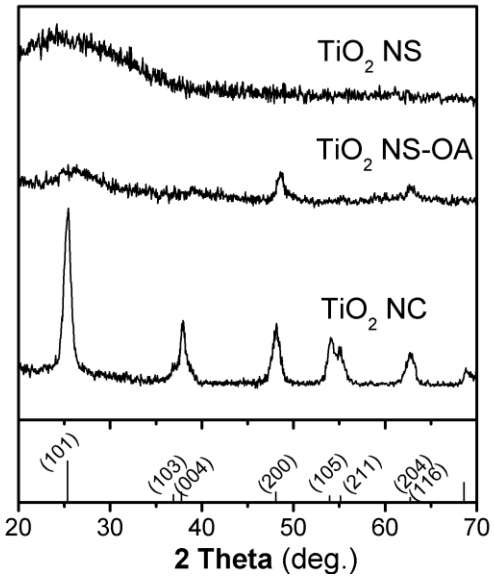

Figure S1. XRD of TiO_2 nanocrystals before exfoliation (NC), nanosheets before exfoliation (NS-OA), and NS after exfoliation (NS). The reference pattern corresponds to anatase TiO_2, JCPDS card #21-1272. After exfoliation, the lamellar ordering of the NS is lost and the lack of long-range order and small NS thickness lead to a featureless XRD pattern. However, the crystallinity of the NS after exfoliation is indicated by the electron diffraction pattern in Figure S3.

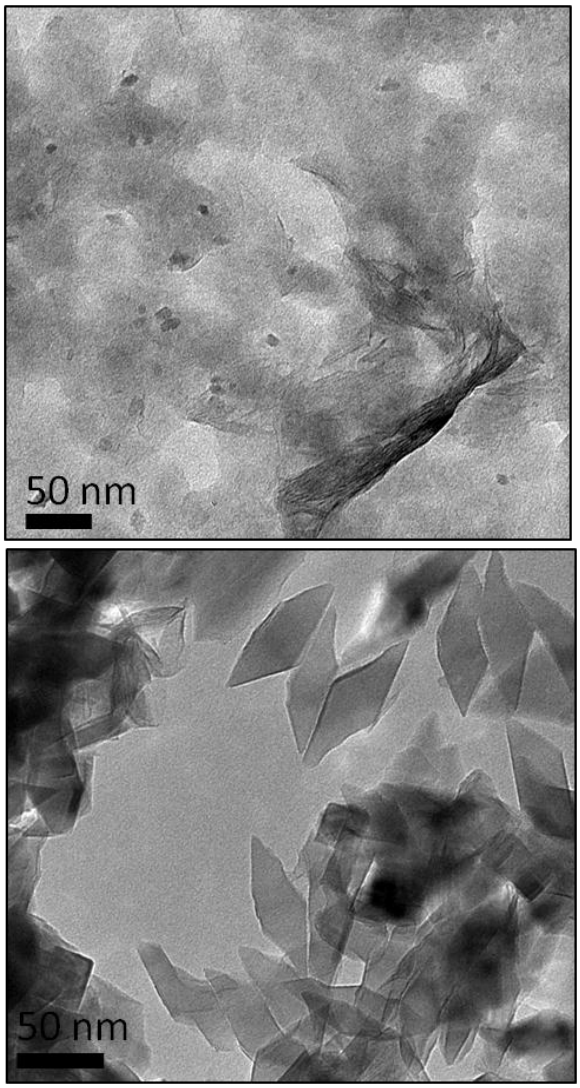

Figure S2. TEM of NS after exfoliaton using TBAOH (top) and TEM of NC after TBAOH treatment (bottom). The NC have a rhombohedral morphology in contrast to that of the nanosheets.

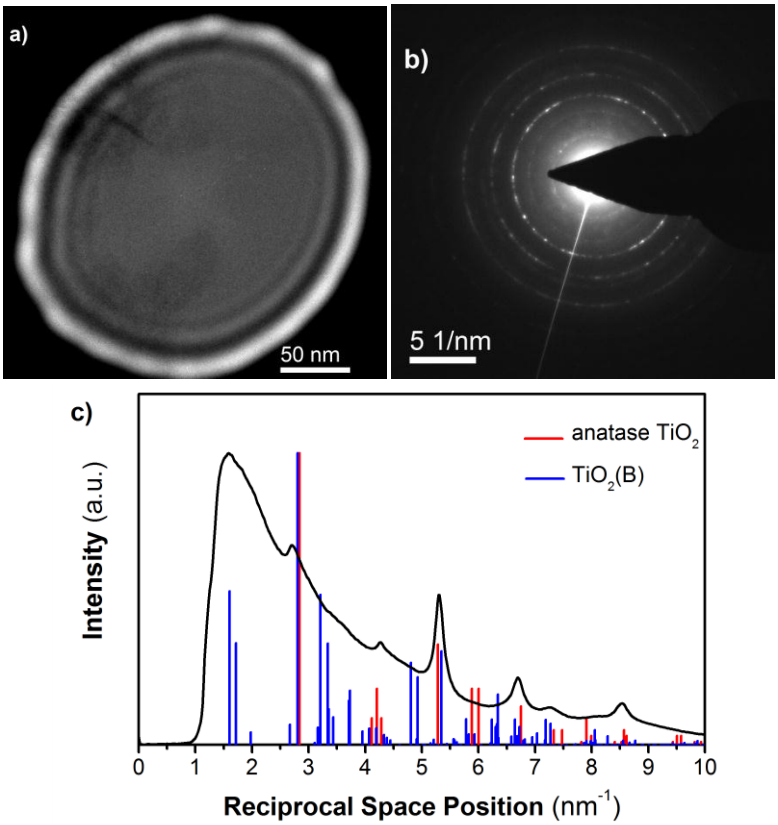

Figure S3. TEM of the TiO_2 NS after exfoliation imaged using a 300 kV electron beam condensed to a small area of the sample with only a few NS: a) real space image, b) electron diffraction of the area shown in (a), and c) plot of diffraction intensity as a function of the reciprocal space position. The expected diffraction peaks for anatase (PDF#00-021-1272) and TiO_2(B) (PDF#01-074-1940) are displayed for reference. The results were calibrated to the (200) and (020) peaks for anatase and TiO_2(B), which occur at 5.285 nm^{-1} and 5.346 nm^{-1}, respectively. Only the anatase reflections match well with all of the observed peaks. The most intense diffraction peak corresponds to the (200) plane of anatase, consistent with the XRD pattern of the NS before exfoliation.

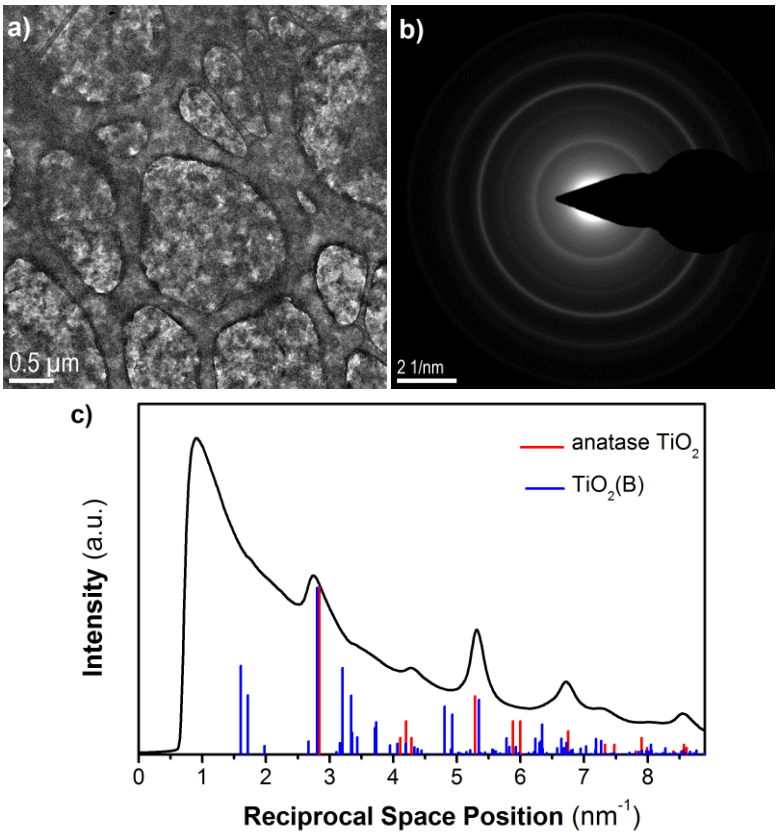

Figure S4. TEM of the TiO_2 NS after exfoliation using a 80 kV electron beam over a large area: a) the real space image, b) the large area electron diffraction pattern and c) the plot of diffraction intensity as a function of the reciprocal space position. The expected diffraction peaks for anatase (PDF#00-021-1272) and TiO_2(B) (PDF#01-074-1940) are displayed for reference. The results were calibrated to the (200) and (020) peaks for anatase and TiO_2(B), which occur at 5.285 nm^{-1} and 5.346 nm^{-1}, respectively. Only the anatase reflections match well with all of the observed peaks, analogous to what was observed in Figure S3. This demonstrates that imaging with a 300 kV electron beam does not affect the structure of the NS.

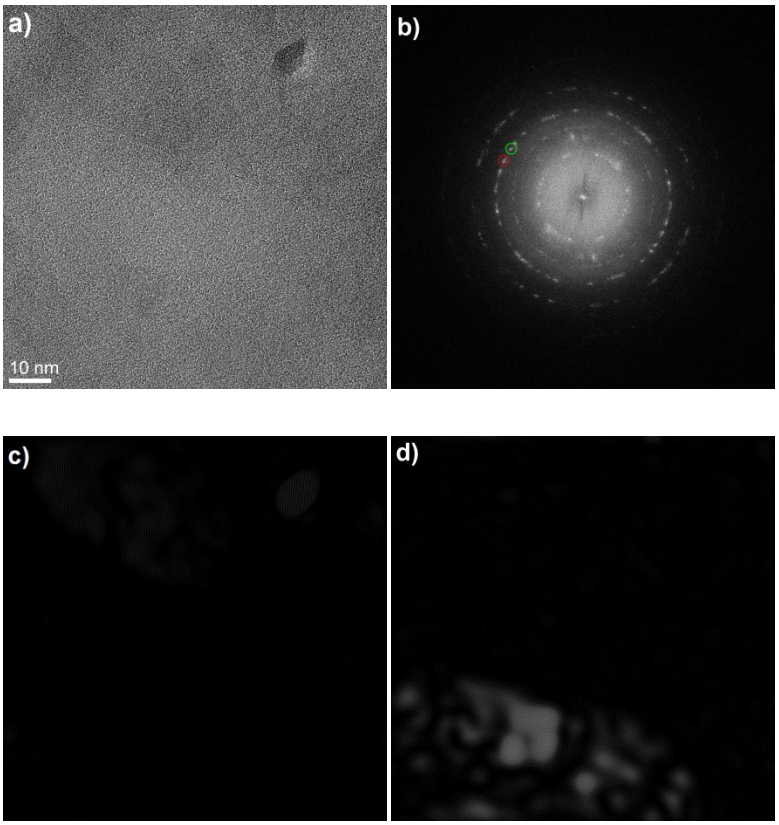

Figure S5. To ensure that the NC impurities in the NS sample were not entirely responsible for the anatase electron diffraction peaks, we applied a filter to the FFT of a HR-TEM image. a) HR-TEM of the NS after exfoliation, b) FFT of the image, c) and d) inverse FFTs of (b) after applying a filter to the spots indicated by the green and red circles, respectively. Filtering separate spots corresponding to the (200) spacing in anatase highlights different crystalline grains in (a).

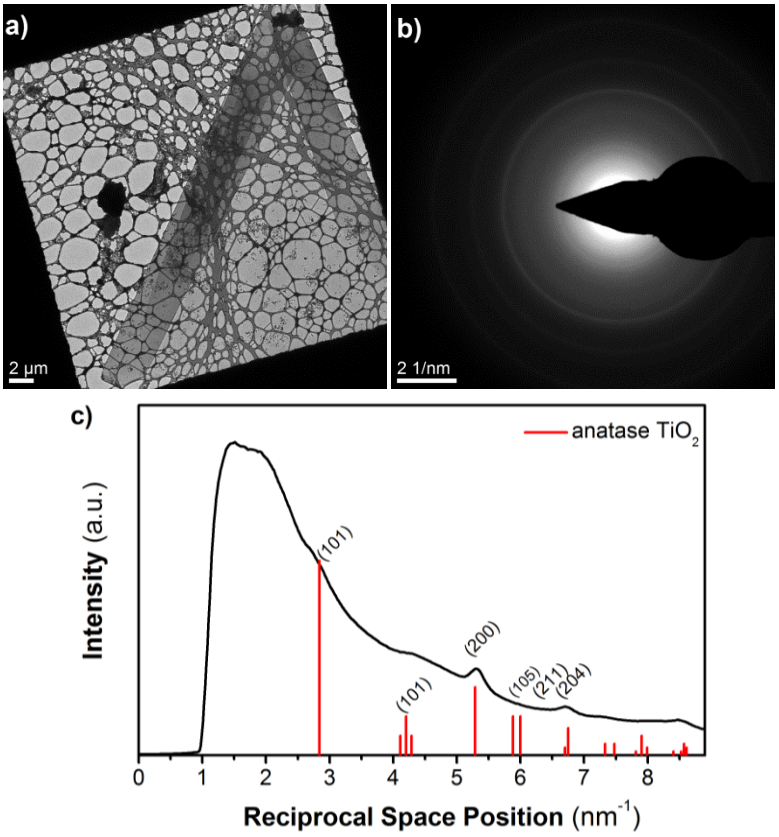

Figure S6. TEM of the TiO_2 NS after exfoliation using a 80 kV electron beam over a large area where the NS lay more flat: a) the real space image, b) the large area electron diffraction pattern from the region where the carbon film on the TEM grid is fully intact in (a), and c) the plot of diffraction intensity as a function of the reciprocal space position. The expected diffraction peaks for anatase (PDF#00-021-1272) and TiO_2(B) (PDF#01-074-1940) are displayed for reference. The results were calibrated to the (200) and (020) peaks for anatase and TiO_2(B), which occur at 5.285 nm^{-1} and 5.346 nm^{-1}, respectively. These results demonstrate that in regions where a few NS are found to lay flat on the TEM grid, the electron diffraction of the (200) anatase peak is the only significant reflection, demonstrating that the NS expose the (001) surface.

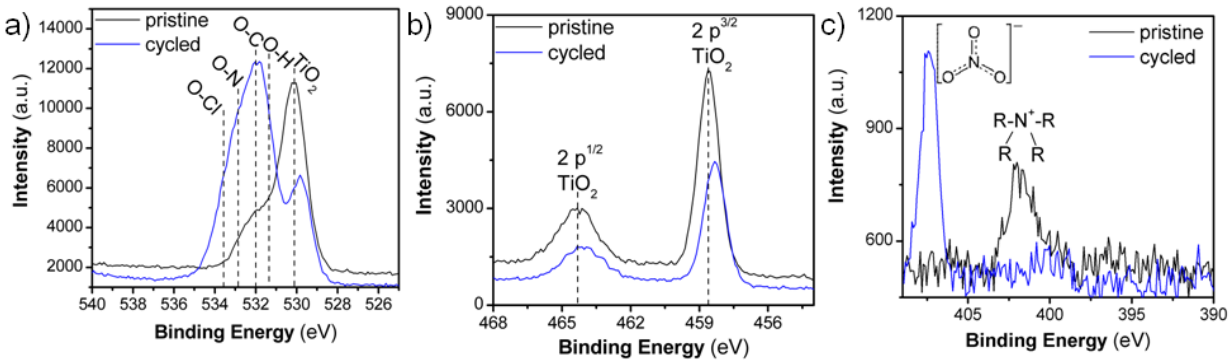

Figure S7. Core XPS spectra of the a) O 1s, b) Ti 2p, and c) N 1s regions of TiO_2 NS before and after cycling in a Li^+ electrolyte at 10 mV s^{-1}.

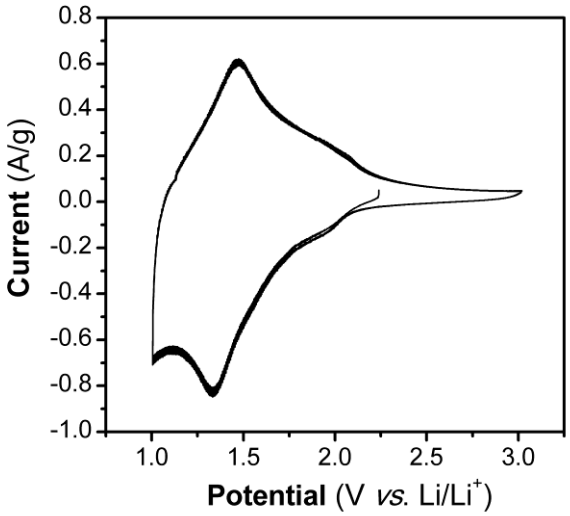

Figure S8. CV at 1 mV s^{-1} for TiO_2 NS in a Li^+ electrolyte for 3 cycles. The peak voltage offset at this rate is 0.14 V.